energies

Article

Heat Transfer during Nitrogen Boiling on Surfaces Modified by Microarc Oxidation

Denis Kuznetsov * and Aleksandr Pavlenko

Kutateladze Institute of Thermophysics, Siberian Branch, Russian Academy of Science, Ac. Lavrentyev Ave., 1, 630090 Novosibirsk, Russia
* Correspondence: kuznetsov_9308@mail.ru

Abstract: Despite the many different methods for creating modified heat transfer surfaces to increase critical heat fluxes and heat transfer coefficients at pool boiling of various liquids at given reduced pressures, active research is currently underway to find optimal surface morphology and geometric parameters of structures for practical application. In this work, we used the method of microarc oxidation (MAO) to obtain coatings with different microstructures on the surface of duralumin heaters. In the present work, we studied the effect of MAO coatings on heat transfer, critical heat flux, and evaporation dynamics during liquid nitrogen boiling under conditions of steady-state heat release at pressures of 0.1, 0.05, and 0.017 MPa. It was shown that the modification of heaters led to a 50–60% increase in heat transfer coefficients as compared to the smooth one under the atmospheric pressure. Based on the data of high-speed video filming of boiling, it was shown that the main mechanism of intensification is the increase in quantity of active nucleation sites. A significant decrease in pressure led to the absence of a significant difference in both heat transfer intensity and evaporation dynamics for the smooth and modified heaters.

Keywords: pool boiling; liquid nitrogen; heat transfer; critical flux; surface modification; microarc oxidation method

Citation: Kuznetsov, D.; Pavlenko, A. Heat Transfer during Nitrogen Boiling on Surfaces Modified by Microarc Oxidation. *Energies* **2022**, *15*, 5792. https://doi.org/10.3390/en15165792

Academic Editor: Daniele Testi

Received: 8 July 2022
Accepted: 8 August 2022
Published: 10 August 2022

1. Introduction

As it is known, to achieve the stable operation of various energy-intensive equipment in the nuclear power industry, chemical industry, heat pump technology, etc., it is necessary to maintain their elements in a certain temperature range. Often, to solve this problem in practice, various liquids with phase transformations, including boiling, are used in heat exchangers, and this is one of the most effective ways of removing heat from a heat-stressed surface. Nevertheless, the rapid development of technologies contributes to an increase in heat flux densities that should be taken from the surface of equipment in operation, including the method of reducing the weight and size parameters of devices. In this regard, in recent decades, the methods used for intensifying heat transfer and increasing critical heat fluxes (CHF) in systems with phase transitions have been comprehensively studied. Today, some of the most promising methods in this field, as it is evidenced by a large number of modern reviews [1–6], are the methods related to the direct modification of heat transfer surfaces by creating various micro/nano-scale structures and coatings on them. Despite the huge number of various liquids, the special attention of researchers is paid to dielectric liquids, which can be used for cooling electronic systems [7].

There are a fairly large number of different physical and chemical methods for surface modification, such as lithography, plasma spraying, mechanical processing, electrodeposition, particle sintering, 3D printing, etc., and each of them has their own advantages and disadvantages. The "method" of mechanical processing for creating intensifying structured surfaces (including microchannels [8] and mesh coatings [9]) has become widespread in the industry due to its simplicity, relative cheapness, scalability, and reproducibility of structures. One of the first works dealt with the effect of structured surfaces consisting of connected internal cavities in the form of tunnels and pores on heat transfer intensity at pool boiling of nitrogen, water, and freon R11 was conducted by Nakayama et al. [10,11]. The authors showed that heat transfer intensification during boiling on such modified surfaces is due to an increase in the proportion of heat by the intensive evaporation of thin liquid menisci between solid and gaseous phases formed during vapor bubble growth and detachment. Further studies of such surfaces with re-entrant channels were associated with varying the shape and geometric parameters of tunnels, pore diameters, reduced pressure (the ratio of operating pressure to the critical pressure of liquid), and type of liquid. The review and systematization of these investigations, including those using commercial surfaces such as Thermoexcel, GEWA, and Turbo, are presented in [12,13].

One of the promising methods of mechanical treatment is the method of deformational cutting (MDC). This technology allows for the creation of complex surfaces with different structures such as spikes or threaded profiles on a macro/micro scale with ultra-dense stacking. The use of such types of structures allows the achievement of six-fold indicators of heat transfer intensification and an increase in critical heat fluxes during water boiling under conditions of free convection [14]. In addition to nucleate pool boiling, the MDC structures showed good results in heat transfer intensification during the film flow of a mixture of freons [15] and nitrogen [16].

Modern and actively developing technologies for creating modified surfaces for the tasks of intensifying heat transfer and increasing critical heat fluxes during boiling include laser surface texturing. Various mechanisms of laser operations such as heating, melting, sublimation, additive manufacturing, etc., can be used for different applications. This method allows for a change in a wide range of parameters of the original surface, such as wettability, roughness, creation of macrostructures and porosity with high accuracy, and reproducibility at various scales. In particular, the effect of the surface modification of cooper heaters by laser treatment on pool boiling of ethanol and water was studied in [17]. The samples had longitudinal grooves of highly developed microstructures with different geometric parameters. As the authors noted, for all the studied samples and liquids, a significant shift of the boiling curves to the region of lower temperature differences was observed in comparison with the data obtained on a smooth heater. Voglar et al. [18] studied the effect of the nanosecond laser texturing of thin stainless steel foil during water boiling. Different patterns in the form of squares, circles, and parallel lines were created on the heaters surfaces. Significantly higher heat transfer coefficients (HTC), up to the factor of 3.7, and critical heat fluxes, up to the factor of 4, were found compared to the unmodified surface. In a subsequent publication [19], the pool boiling of water, ethanol and their mixtures on stainless steel foils modified with a pulsed fiber laser were investigated. In [20], a silicon substrate modified by laser ablation was used to intensify heat transfer during pool boiling of water. It was shown that the HTC for the laser treated sample was up to 49.5% higher compared to the untreated one and up to 234% higher compared to the polished sample. The authors noted that laser texturing led to a significant increase in the nucleation site density (NSD) and nucleation frequency, while the departure diameters of bubbles on the modified surface decreased significantly. The generalization and systematization of publications related to the modification of surfaces by the method of laser texturing in relation to the problems of intensifying heat transfer in systems with phase transitions are presented in [21].

A high degree of heat transfer intensification and an increase in CHFs during boiling can be achieved by creating porous coatings by the method of sintering. An important advantage of coatings obtained by this technology is high porosity, which allows not only an increase in the effective heat releasing surface area, but also the facilitation of the nucleation process (initiation of vapor formation at lower temperature difference, increasing the nucleation site density). One example of industrial application of this method is commercial High-flux tubes, the use of which leads to the intensification of heat transfer during boiling by a factor of 3–20 [12,22]. In addition, sintering allows for the creation of 2D and 3D highly porous coatings of various geometries. For example, in [23–25], the effect of porous coatings in the form of cones and ridges uniformly distributed over the heater surface was studied for various microstructural parameters of the coating. The authors were able to achieve a 10-fold increase in heat transfer and a 3-fold increase in the value of critical fluxes compared to the unmodified heater when boiling n-pentane. Based on the hydrodynamic theory of crisis development during boiling, a model that predicts the CHF magnitude on similar structured coatings depending on the wavelength of structure modulation was constructed. Nevertheless, the method of sintering has some disadvantages, such as the complexity of applying coatings on surfaces of different shapes and the complexity of manufacturing associated with the need to achieve high temperatures and pressures. A modern alternative is the method of directional plasma spraying [26], which allows the creation of 3D capillary-porous coatings with a high porosity. The issues of intensification HTC during the boiling of water and liquid nitrogen on tubular heaters modified by this method were considered in [27–29]. The authors managed to achieve a three-fold increase in heat transfer compared to the smooth surface in the region of low heat fluxes. Moreover, it was found that the presence of such coatings on heater surfaces leads to the degeneration of the nonstationary critical heat flux in liquid nitrogen during an impulsive increase in the heat load, and the rapid transition to film boiling occurs at a heat release rate twice as high as that at of the stationary CHF.

Many researchers have recently shown an increased interest in the development and study of anisotropic coatings that consist of areas with contrasting wettability [30], different thermal conductivity [31], porosity, and multiscale structuredness [32,33], mainly to modulate effectively the two-phase flow at boiling with the aim of HTC and CHF intensification. Despite the large number of works devoted to the study of the effect of surface modification by various methods on heat transfer and crisis phenomena in systems with phase transitions, today an active search is underway for optimal microstructural parameters, materials, and geometry of the resulting functional surfaces, as well as commercially profitable technologies for given regime parameters of the system.

One of the promising ways to create porous coatings with a thickness from fractions to hundreds of micrometers is the method of microarc oxidation (MAO), which has been known since the late 1970s. The coatings obtained by this method are porous ceramics of a complex composition, formed due to metal surface oxidation and the inclusion of electrolyte elements in the coating composition. This technology is widely used in the industry because the resulting oxide films have good electrical insulation properties and corrosion and wear resistance. The main advantages of the MAO method for creating functional surfaces in relation to the task of increasing HTC and CHF are scalability, the possibility of applying coatings to substrates of complex geometry, a high degree of coating adhesion, and relative cheapness in production. Despite this, there are almost no publications that deal with the study of heat transfer features and the development of crisis phenomena during the boiling of various liquids on the MAO coatings with varying micromorphological characteristics of the structure. In particular, [34] presented the results of an experimental study of heat transfer during liquid nitrogen and freon 113 boiling on spheres with ceramic coatings at atmospheric pressure under conditions of free convection. It has been found that the formation of porous coatings on the surface by the method of microarc oxidation leads to a reduction in the time of their cooling, the deformation of boiling curves, and an increase in the temperature of film boiling termination. Vasil'ev et al. [35] investigated features of heat transfer during the boiling of subcooled water on a titanium foil modified by microarc oxidation with deposition of aluminum oxide particles from the nanofluid. The presence of such a coating led to heat transfer intensification by 20–30%. The authors of [36] studied heat transfer during film cooling of a bundle of horizontal tubes with MAO coatings deposited using various electrolytes. A three-fold increase in HTC, compared to the uncoated tube, was achieved.

The aim of this work was to study the effect of coatings obtained by microarc oxidation on heat transfer during nitrogen boiling under conditions of steady-state heat release at natural convection on flat heaters under reduced pressures in the range of 0.005–0.029.

2. Materials and Methods

The scheme of the experimental setup, the main elements of which are described in [37], and the test section for studying heat transfer during pool boiling are shown in Figure 1. The working fluid was liquid nitrogen, obtained using a Cryomech LNP120 liquefaction plant, which supplied liquid nitrogen with a purity of 99.9% or higher. The free escape of excess vapors was carried out through the vapor outlet on the top of the cryostat that can be blocked using a valve. The experiments were carried out at three reduced pressures, 0.029, 0.015, and 0.005 (0.1, 0.05, and 0.017 MPa respectively). To achieve a low pressure in the working volume, a connector was installed in the upper flange with a connected cryogenic pipeline, leading to a vacuum pump that pumps out liquid nitrogen vapor. The pressure inside the cryogenic volume was controlled by a reference vacuum gauge that could record the measurements with an accuracy of 0.005 kgf/cm^2. A given level of reduced pressure during the nitrogen boiling in experiments was maintained by changing the rate of vapor pumping out using a fine-tuning valve installed on the pump. The maximum decrease in pressure during nitrogen boiling due to a change in the liquid level did not exceed 2.5%.

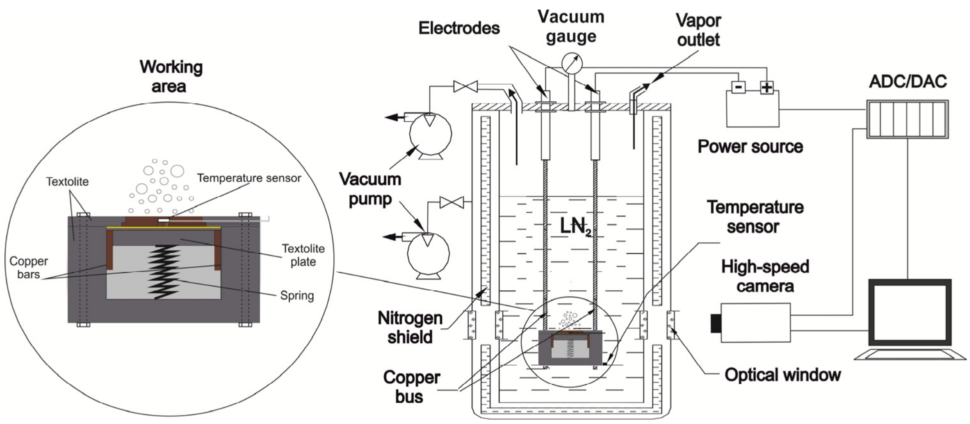

Figure 1. Scheme of the experimental setup and test section.

The plates made of duralumin D16T with roughness R_a = 1 µm (average roughness), R_z = 7.1 µm (maximum height to minimum depth), dimensions of 22 × 22 mm, and a thickness of 3 mm were used as the working samples. It should be noted that the samples were made on a milling machine and were not subjected to further processing (grinding, polishing); therefore, the heat transfer surface had a specific microstructure characteristic of technical surfaces. A groove was made along the perimeter of each working sample to connect the section with the textolite body (see the test section scheme, Figure 1). The textolite body, consisting of two halves, was connected with four bolts. To exclude liquid inflows in the test section, all component parts of it were sealed with epoxy glue. The Hel-700 series pre-calibrated platinum resistance temperature detector (RTD) was installed in the center of each sample at a distance of 0.5 mm from the heat releasing surface, which allowed surface temperature measurements with an absolute error not exceeding 0.2 K. A thin layer of highly heat conductive thermal paste (11 W/mK) was applied between the sensor body and the test sample to ensure good thermal contact, and epoxy adhesive was used to fix the sensor securely. The RTD was connected in a four-wire circuit by constantan wires 90 µm in diameter, laid in a 2.5 mm deep groove, located from the test sample center to the outer edge of the textolite frame. Thin constantan wires, as well as the use of a REF200 precision current generator to power the sensor, allowed the minimization of both the heat sink through the measuring wires and the thermometer resistance measurement error associated with the sensor self-heating. The same RTD was used to determine the temperature of the working volume of liquid nitrogen. The distance between the sensor and heating surface was about 5 cm, sufficient to exclude the effect of the boiling process on thermometer readings.

To heat the sample, the electric current was passed through a 50-μm thick constantan foil soldered to copper terminals using a GORN-K-12/600 programmable power supply. A thin mica gasket with a 50-μm thickness was used to exclude electrical contact between the constantan foil and duralumin sample. The heat release power was determined from the voltage readings at the current-carrying terminals at a given level of current from power supply. The error in measuring the heat flux density q was calculated from the accuracy of measuring the voltage, current, and heat transfer area and did not exceed 4%. To ensure good thermal contact between duralumin and constantan, the foil was pressed by spring and textolite plate. The experiments were carried out both with an increase in q and with a decrease (from the value of heat flux slightly lower than the critical one).

All measurements, as well as control of the heat release power, were made using the NI 6251 ADC/DAC board and the LabView software package. Registration of the boiling process was carried out with a high-speed video camera, Phantom VEO 410, through optical windows of the setup.

To perform the experiments on studying heat transfer during nitrogen boiling, various coatings were fabricated on the test sample surface by the method of microarc oxidation [38]. The essence of this method lies in the fact that samples of metals (Al, Mg, Ti, Zr, Nb, Ta, etc.) and their alloys, together with the cathode, are immersed in an electrolyte solution and are exposed to a high-density electric current (significantly higher than that at anodizing). When such a current passes through the "metal-electrolyte" interface, chaotic microplasma discharges with high temperatures are created on the surface of a part. These micro-discharges have plasma-chemical and thermal effects on the coating and electrolyte. At the discharge site, a film is created from oxidized forms of the base metal and electrolyte components. Using this method, it is possible to create coatings with different microstructures and thicknesses by changing the composition of the electrolyte, current density, pulse duration, processing time, etc. It should be noted that, in the temperature range of 80–100 K, close to the boiling point of liquid nitrogen at atmospheric pressure, the thermal conductivity of Al_2O_3 (material of the samples in this study is duralumin) is about 400 W/mK [39], which exceeds the thermal conductivity of duralumin. In this regard, the resulting coatings do not introduce an error in the measurement of the temperature of heat releasing surface. Two heaters with MAO coatings were used in the experiments:

Sample No. 1: electrolyte − KOH 4 g/L + sodium liquid glass of 8 g/L; anode/cathode currents of 24/24 A/dm^2; pulse rate of 1500 Hz; processing time of 10 min.

Sample No. 2: electrolyte − $Na_5P_3O_{10}$ 20 g/L; anode/cathode currents of 5/3 A/dm^2; pulse rate of 500 Hz; processing time of 40 min.

The surface structure of both the uncoated heater and the samples modified by the MAO method was analyzed using a Hitachi S-3400N scanning electron microscope (SEM). Coating thickness was determined using energy-dispersive X-ray spectroscopy (EDX) of the sample cross-section. To determine the roughness of samples, a BRUKER Contour GT-K1 optical interference profilometer was used. The SEM photographs, as well as the phase maps of elements in the crosscut, which allow for determining the distribution of the thickness of obtained coatings over the heater, are presented in Figure 2. As it can be seen, the surface of the uncoated heater (smooth heater) consists of regularly alternating grooves made by the milling machine. The coating of sample No. 1 is a rough surface (R_a = 3.4 μm, R_z = 26 μm) with individual pores 2–5 μm in diameter, and the coating thickness varies in the range of 2–20 μm (the oxide layer, i.e., the layer of the formed coating, is highlighted in blue in the figure). Much more pronounced porosity is observed on the surface of sample No. 2 with a high density of pores; however, their sizes are much smaller than those of sample No. 1 and lie in the range of 1–2 μm, and the roughness is R_a = 3.7 μm, R_z = 28 μm. The coating thickness is also significantly lower for sample No. 2 and amounts to 1–6 μm.

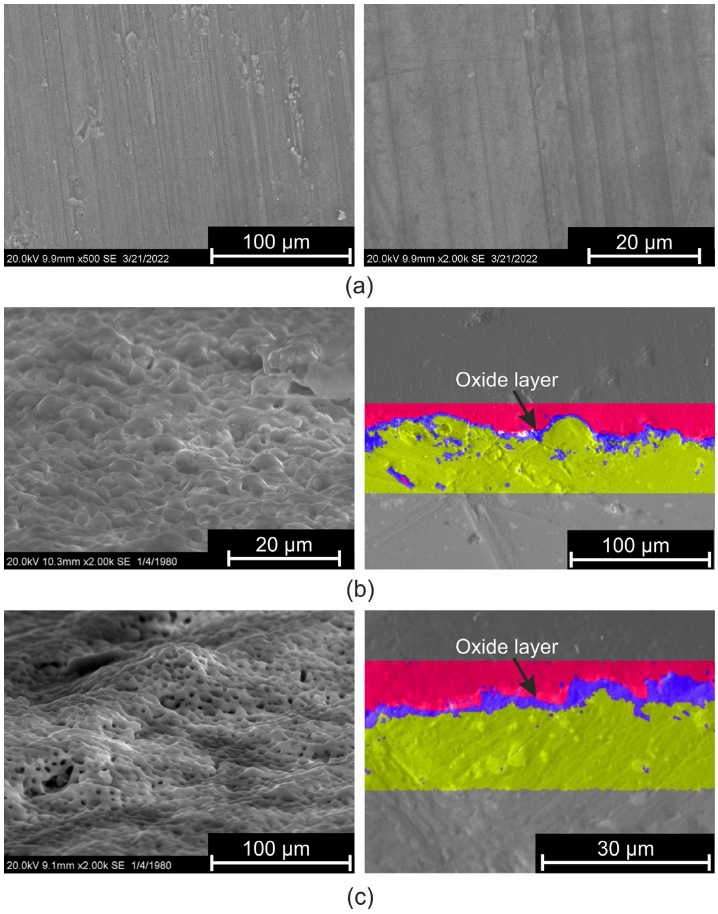

Figure 2. Structure of the heaters: (**a**) SEM of the smooth sample; (**b**) SEM and EDX of sample No. 1; (**c**) SEM and EDX of sample No. 2.

3. Results and Discussion

To study heat transfer and crisis phenomena during liquid nitrogen boiling at the saturation line at the atmospheric and two low pressures (p = 0.05 and 0.017 MPa) under conditions of steady-state heat release, the experiments were carried out on two test samples modified by the MAO method and a heater without coating. For all heaters, several series of experiments were carried out, both with an increase in the heat load and with its decrease. The heat flux was changed by a small discrete value, and with each change in the heat release power, several tens of minutes were waited to ensure stationary conditions for the experiments. It should be noted that hysteresis of the boiling curve was observed to some extent for all test samples. At the same time, with a decrease in the heat release power, the experimental data of different series obtained for each individual sample coincided with good accuracy. All heat transfer data below were obtained under the conditions of reduced heat load.

The boiling curves, as well as values of critical heat fluxes q_{cr} for the uncoated heater, are presented in Figure 3 for all investigated pressures. A characteristic break in the curve was observed for each dependence at a heat flux of about 1 W/cm^2; it corresponds to the transition between convection and developed nucleate boiling. A decrease in pressure in the working section leads to a shift of this transition to the region of higher temperature differences. The value of the CHF was determined in experiments both by a rapid increase in the temperature of the heat-releasing surface and by the formation of a continuous vapor film along the heater during boiling visualization. For this test sample under the studied pressures, it is q_{cr} = (18.2; 13.5; 11.5) W/cm^2, respectively, and it is in good agreement with the well-known Kutateladze-Zuber model [40,41] at a coefficient of 0.14 under the pressures of 0.1 and 0.05 MPa. At the lowest pressure in the experiments, the experimental data on the CHF value were somewhat higher than the theoretical dependence. In addition, at 0.017 MPa, a significant decrease in the heat transfer intensity (up to 30%) relative to the atmospheric pressure was obtained in the entire region of heat loads. At the same time, at 0.05 MPa, a decrease in HTC does not exceed 10%, and in the region of moderate and high heat fluxes, the heat transfer coefficient is even slightly higher than that at an atmospheric pressure. Multiple repeated experiments for data verification show similar results. Such an anomalous behavior of the boiling curve (nonmonotonic dependence on pressure) relates possibly to the peculiarities of hydrodynamics of the process on a heater with a specific surface microstructure (mentioned earlier), but the determination of more precise causes requires a separate study.

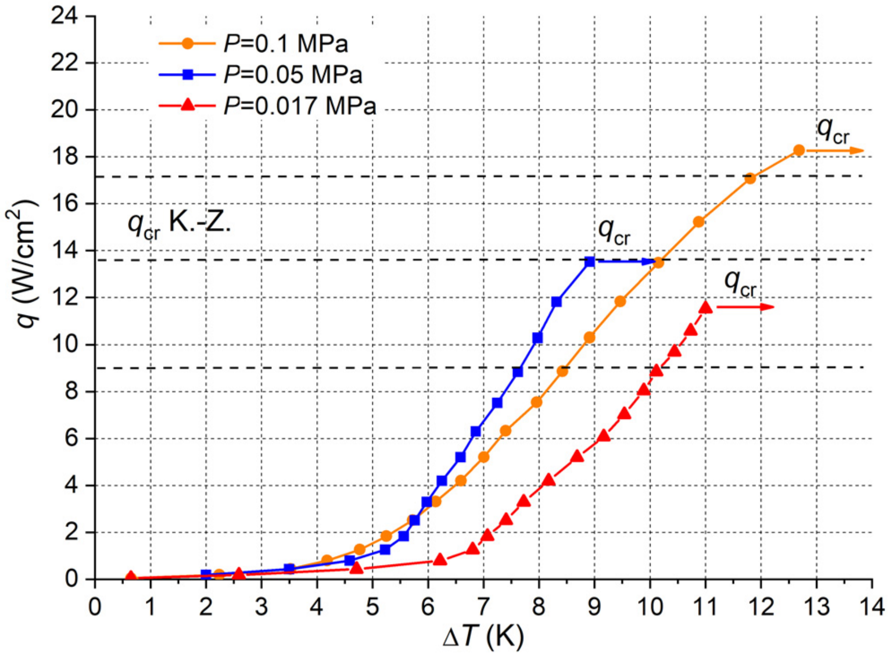

Figure 3. Boiling curves for the smooth heater at different pressures.

The boiling curves, as well as values of critical heat fluxes, for the samples modified by microarc oxidation at all studied pressures are shown in Figure 4. For sample No. 1, there is no pronounced break in the curve at atmospheric pressure, which is due, as it will be shown below, to boiling with a high nucleation site density even at very low heat fluxes (less than 0.4 W/cm^2). In addition, for this sample, the critical heat fluxes obtained during the experiments almost coincide with the CHF for the uncoated sample both at atmospheric and low pressures and are q_{cr} = (17.5; 13.4; 11.2) W/cm^2, respectively. For sample No. 2, we can see a slight decrease by 15% (15.4 W/cm^2) in the critical heat flux compared with the uncoated heater at atmospheric pressure, but there is almost no effect of the coating on the CHF (12.7 and 11.6 W/cm^2) at pressures of 0.05 and 0.017 MPa. A decrease in pressure during experiments leads to degradation in the heat transfer on both modified heaters and a shift in the transition from natural convection to developed nucleate boiling to the region of higher temperature differences. The maximum decrease in heat transfer at 0.05 MPa was 30% for both test samples, and it was 55% and 45% for the samples No. 1 and No. 2, respectively, at 0.017 MPa.

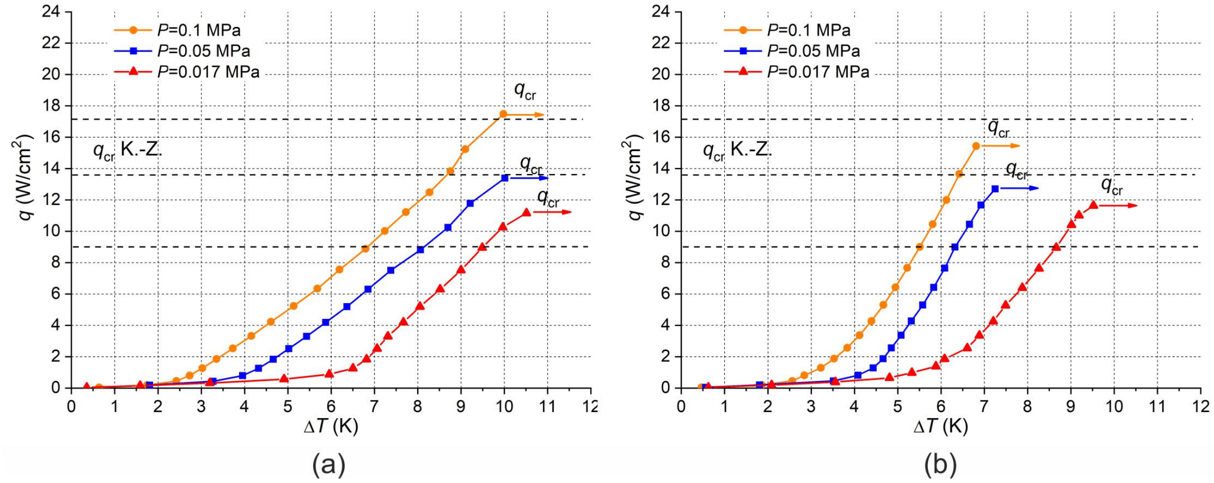

Figure 4. Boiling curves for the modified heaters at different pressures: (**a**) sample No. 1; (**b**) sample No. 2.

The enhancement factors (the ratio of the HTCs on the modified heaters to the same value for the uncoated heater at the fixed heat flux values) are shown in Figure 5. Thus, for sample No. 1, we can see a significant degree of heat transfer intensification up to 60% at atmospheric pressure in the region of low q, which decreases with increasing heat release power. At a pressure of 0.05 MPa, the maximum increase in heat transfer coefficients was much lower (up to 20%), approaching the measurement error, and it was also obtained at low heat fluxes. At the same time, the trend towards a decrease in heat transfer intensification persisted and, at $q > 6$ W/cm^2, leads at $p = 0.05$ MPa to even a slight deterioration in heat transfer relative to the uncoated heater. With a maximum decrease in operating pressure, the coating on the heater surface, obtained by microarc oxidation using potassium hydroxide as an electrolyte, did not affect heat transfer in the entire studied range of heat fluxes up to the heat transfer crisis.

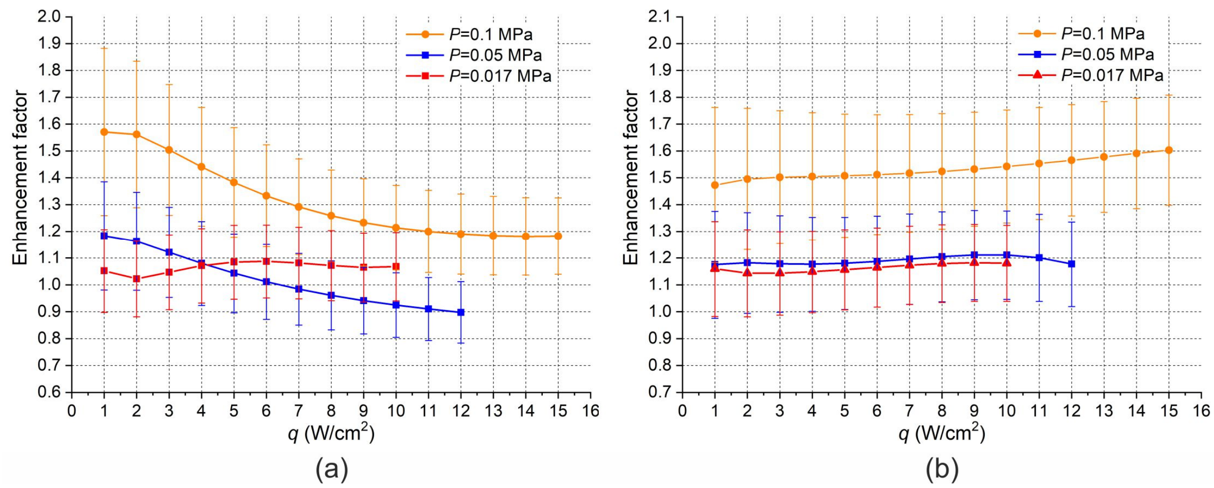

Figure 5. Intensification of heat transfer at different pressures: (**a**) sample No. 1; (**b**) sample No. 2.

A different dependence of the heat transfer coefficients on the heat flux density was observed for MAO coating No. 2. Under atmospheric pressure, the presence of such a coating on the heat transfer surface led to heat transfer intensification by 50–60%, while this value hardly changed with a change in the heat flux until the heat transfer crisis. This trend can be related to small diameters of coating pores (of about 2 μm), which are gradually activated when certain overheating of the heat-releasing surface is achieved with a heat flux increase. In addition, the formation of a vapor bubble on the heat transfer surface reduces the local temperature near this particular site and, due to the high pore density of such a coating, hampers the activation of adjacent pores. For sample No. 2, there is almost no heat transfer intensification at low pressures, which is close to the measurement error. A qualitative analysis of the video presented below showed a significant increase in the nucleation site density on MAO coatings at atmospheric pressure in the region of heat loads $q < 1$ W/cm^2, which, apparently, is the main reason for heat transfer intensification. As it is known, various microcavities (recesses, pores, cracks, etc.) are the active evaporation sites during liquid boiling on a solid surface. The quantity that determines the minimum dimensions of such irregularities is the critical nucleation radius [42]:

$$R_c = 2\sigma T_{sat}/(L\rho_v \Delta T),$$

where σ is the surface tension coefficient, L is the specific heat of vaporization, ρ_v is the vapor density, and ΔT is the temperature difference (surface of the heater and saturation of nitrogen). The analysis of this relationship shows that for liquid nitrogen at an overheating of 1 K under atmospheric pressure, this value is 1.5 μm, and it is comparable with the pore sizes on MAO coatings. However, a decrease in pressure leads to a significant increase in this value (by a factor of 5 at a pressure of 0.017 MPa). As a result, pores of the same size as the studied coatings in the region of low pressures almost do not affect the boiling process, and this explains the absence of heat transfer intensification for heaters No. 1 and No. 2. Thermophysical properties of liquid nitrogen as a function of pressure were taken from the data [43].

A high-speed video of the boiling process was carried out at all studied pressures and heat fluxes, the frames of which are presented in Figures 6–8. It should be noted that the peculiarity of the test section design led to the appearance of edge effects in the area of contact between the epoxy sealant and the test sample. Namely, it is liquid boiling along the flat heater perimeter at low heat fluxes, which, in combination with side video recording and a large number of boiling centers on the heat transfer surface, significantly complicates the collection of statistics on the magnitude of the separation diameters of individual bubbles and does not allow a quantitative assessment of the nucleation site density. According to the qualitative analysis of the video, at heat fluxes $q < 1$ W/cm^2 at atmospheric pressure, the density of active vaporization sites on the heaters with coatings significantly exceeds the similar value for a smooth heater. The reason is that pores can act as vapor traps that increase the amount of residual vapor in the active site after bubble departure, facilitating the formation of a new vapor bubble and ensuring the stability of boiling centers. In addition, for sample No. 1, boiling with a high nucleation site density was observed even at a very low heat flux of 0.4 W/cm^2, while the bubble departure diameters were about 100 μm. This explains the absence of a characteristic break in the obtained boiling curve for this heater at atmospheric pressure. For sample No. 2, boiling was also observed at this heat flux, but with a much lower density of vaporization sites, and, therefore, the convective component made a significant contribution to the heat transfer. The departure diameters of bubbles from individual sites at a given heat release rate varied from 100 to 500 μm. On the heater with a coating at such a low heat load, only single active sites (of about 10–15) with bubble departure diameters of 350–600 μm were observed over the entire heat transfer surface. A decrease in the departure diameters of bubbles during liquid boiling on porous surfaces relative to the data obtained on smooth samples is noted in many papers, for example [44,45]. At low pressures, no significant difference in boiling on a heater without coating and modified samples was observed in the entire range of heat loads. In this case, the departure diameters of bubbles increased significantly (bubbles up to 5 mm in diameter were detected at 0.017 MPa), and the nucleation site density decreased relative to atmospheric pressure at similar fixed values of the heat flux.

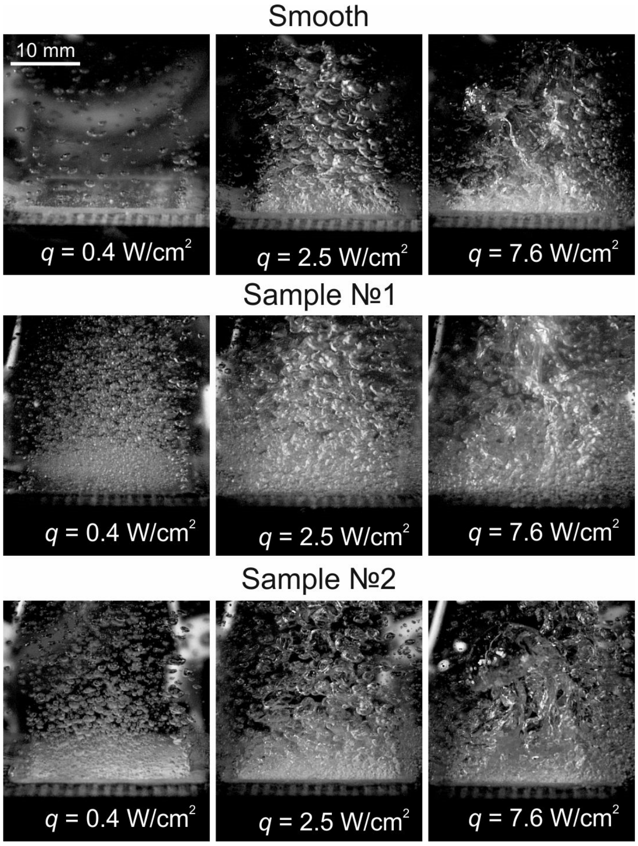

Figure 6. Boiling process at atmospheric pressure.

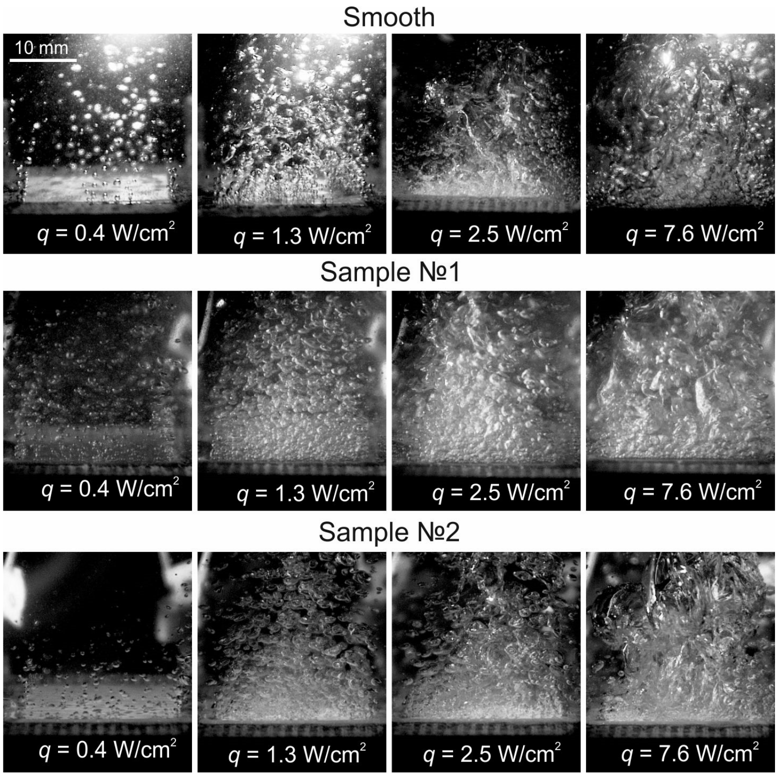

Figure 7. Boiling process at 0.05 MPa.

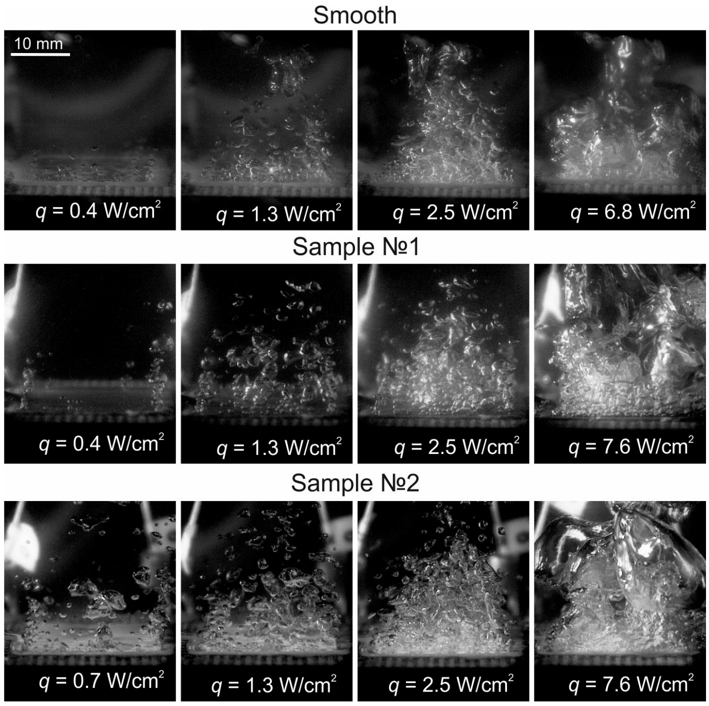

Figure 8. Boiling process at 0.017 MPa.

Despite the achieved heat transfer intensification during nitrogen boiling on the studied MAO coatings, as well as the widespread use of this method to create wear-resistant, electrically insulating elements of various devices, today there is a variety of other methods for creating coatings on heat transfer surfaces in relation to the problem of intensifying heat transfer and increasing critical heat fluxes during boiling, including cryogenic liquids. Figure 9 compares the results of heat transfer intensification during liquid nitrogen boiling at atmospheric pressure obtained in this study and other works (on porous surfaces). As it can be seen, the data presented in [46] for the tubular heaters with a 22-mm diameter with aluminum coatings and a porosity of 20–30%, fabricated by the traditional plasma spraying method, are close to the results of this work in the region of low heat fluxes (maximum intensification is about 50%). An increase in the heat flux leads to a decrease of the enhancement factor, and at q~3 W/cm^2, there is no difference in HTC compared to the uncoated tube. Much better results have been achieved in [37] by boiling liquid nitrogen on structured capillary-porous coatings with a porosity of 30% obtained by selective laser melting/sintering SLM/SLS. These coatings are characterized by regular ridges and channels with a sinusoidal dependence of the two-dimensional cross-section profile. An almost six-fold increase in heat transfer intensity in comparison with a smooth heater at atmospheric pressure was obtained, as well as a 30% increase in the critical heat flux. Such values of intensification were achieved due to a significant increase in the NSD and the heat transfer area, as well as the effective modulation of a two-phase countercurrent flow near the heat-releasing surface. It is also worth noting that a three-fold intensification, apparently associated with a wide range of pore sizes for such coatings, was obtained at a pressure of 0.018 MPa in [37]. Even higher values were achieved in [47], where the authors used plasma spraying to obtain aluminum coatings on the plate heaters. They significantly increased the porosity of modified samples, compared to the traditional plasma spraying method by adding polyester to the depositing powder, with subsequent decomposition and evaporation of this component at high temperature air.

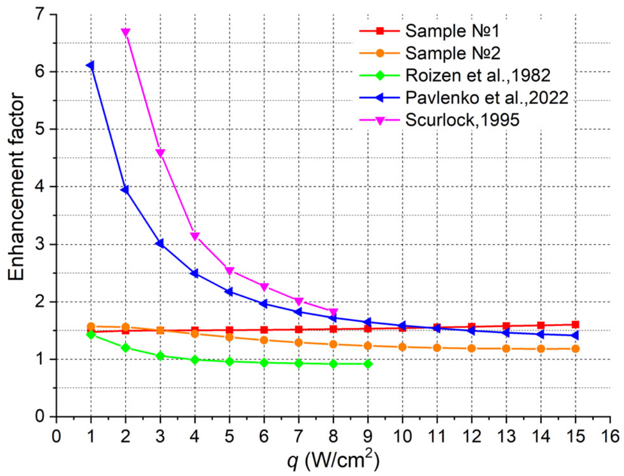

Figure 9. Comparison of data from various studies on the heat transfer enhancement during nitrogen boiling on modified heaters at atmospheric pressure.

4. Conclusions

In the present investigation, experimental results on the effect of porous coatings of various microstructures obtained by microarc oxidation on heat transfer during liquid nitrogen boiling at different reduced pressures in the range of 0.005–0.029 are presented.

It is shown that:

- At atmospheric pressure, such coatings lead to heat transfer intensification by 50–60%, compared to a smooth sample. At that, for a coating with a high pore density obtained using sodium tripolyphosphate as an electrolyte, the intensification value hardly changed with a change in the heat flux, while for the second modified sample (potassium hydroxide as an electrolyte), there was a tendency towards a decrease in intensification with an increase in heat release power.
- At all studied pressures, there was no significant effect of MAO coatings on the critical heat flux value, as well as on heat transfer intensity at low pressures (0.05 MPa and 0.017 MPa), compared to the smooth sample.
- The main mechanism for increasing the heat transfer coefficients on modified samples at atmospheric pressure was an increase in the nucleation site density. A decrease in pressure minimized the difference in evaporation dynamics on the smooth and modified heaters, led to an increase in the temperature difference at which the transition from convection to developed nucleate boiling occurs, and increased the departure diameters of bubbles.
- Based on a comparison with the data of other works, it was established that highly porous and structured coatings are the more effective coatings in relation to the problem of intensifying heat transfer and increasing critical heat fluxes during nitrogen boiling. However, their use has great advantages in intensifying heat transfer at low and moderate heat flux densities ($q < 8$ W/cm^2~0.4–0.5 q_{cr}).

Author Contributions: Both authors made a significant contribution to the preparation and writing of the article; preparation and conduct of the experiments as well as processing of the results was performed by D.K.; statement of the research problem, review, and editing was performed by A.P. All authors have read and agreed to the published version of the manuscript.

Funding: This research was funded by the project of the Russian Federation represented by the Russian Ministry of Education and Science (agreement No. 075-15-2020-770).

Institutional Review Board Statement: Not applicable.

Informed Consent Statement: Not applicable.

Data Availability Statement: The data presented in this study are available on request from the corresponding author.

Conflicts of Interest: The authors declare no conflict of interest.

References

1. Dedov, A.V. A Review of Modern Methods for Enhancing Nucleate Boiling Heat Transfer. *Therm. Eng.* **2019**, *66*, 881–915. [CrossRef]
2. Liang, G.; Mudawar, I. Review of Pool Boiling Enhancement by Surface Modification. *Int. J. Heat Mass Transf.* **2019**, *128*, 892–933. [CrossRef]
3. Volodin, O.A.; Pecherkin, N.I.; Pavlenko, A.N. Heat Transfer Enhancement at Boiling and Evaporation of Liquids on Modified Surfaces. *High Temp.* **2021**, *59*, 280–312. [CrossRef]
4. Mahmoud, M.M.; Karayiannis, T.G. Pool Boiling Review: Part II–Heat Transfer Enhancement. *Therm. Sci. Eng. Prog.* **2021**, *25*, 101023. [CrossRef]
5. Chen, J.; Ahmad, S.L.; Cai, J.; Liu, H.; Lau, K.T.; Zhao, J. Latest Progress on Nanotechnology Aided Boiling Heat Transfer Enhancement: A Review. *Energy* **2021**, *215*, 119114. [CrossRef]
6. Shojaeian, M.; Kosar, A. Pool Boiling and Flow Boiling on Micro-and Nanostructured Surfaces. *Exp. Therm. Fluid Sci.* **2015**, *63*, 45–73. [CrossRef]
7. Sajjad, U.; Sadeghianjahromi, A.; Ali, H.M.; Wang, C.C. Enhanced Pool Boiling of Dielectric and Highly Wetting Liquids–A Review on Surface Engineering. *Appl. Therm. Eng.* **2021**, *195*, 117074. [CrossRef]
8. Kaniowski, R.; Pastuszko, R. Pool Boiling of Water on Surfaces with Open Microchannels. *Energies* **2021**, *14*, 3062. [CrossRef]
9. Zhang, S.; Jiang, X.; Li, Y.; Chen, G.; Sun, Y.; Tang, Y.; Pan, C. Extraordinary Boiling Enhancement through Micro-Chimney Effects in Gradient Porous Micromeshes for High-Power Applications. *Energy Convers. Manag.* **2020**, *209*, 112665. [CrossRef]
10. Nakayama, W.; Daikoku, T.; Kuwahara, H.; Nakajima, T. Dynamic Model of Enhanced Boiling Heat Transfer on Porous Surfaces. I. Experimental Investigation. *Trans. ASME J. Heat Transf.* **1980**, *102*, 445–450. [CrossRef]
11. Nakayama, W.; Daikoku, T.; Kuwahara, H.; Nakajima, T. Dynamic Model of Enhanced Boiling Heat Transfer on Porous Surfaces. II. Analytical Modeling. *Trans. ASME J. Heat Transf.* **1980**, *102*, 451–456. [CrossRef]
12. Ribatski, G.; Thome, J.R. Nucleate Boiling Heat Transfer of R134a on Enhanced Tubes. *Appl. Therm. Eng.* **2006**, *26*, 1018–1031. [CrossRef]
13. Mehta, J.S.; Kandlikar, S.G. Pool Boiling Heat Transfer Enhancement Over Cylindrical Tubes with Water at Atmospheric Pressure, Part I: Experimental Results for Circumferential Rectangular Open Microchannels. *Int. J. Heat Mass Transf.* **2013**, *64*, 1205–1215. [CrossRef]
14. Shchelchkov, A.V.; Popov, I.A.; Zubkov, N.N. Boiling of a Liquid on Microstructured Surfaces under Free-Convection Conditions. *J. Eng. Phys. Thermophys.* **2016**, *89*, 1152–1160. [CrossRef]
15. Volodin, O.A.; Pecherkin, N.I.; Pavlenko, A.N.; Zubkov, N.N. Surface Microstructures for Boiling and Evaporation Enhancement in Falling Films of Low-Viscosity Fluids. *Int. J. Heat Mass Transf.* **2020**, *155*, 119722. [CrossRef]
16. Kuznetsov, D.V.; Pavlenko, A.N.; Volodin, O.A. Effect of Structuring by Deformational Cutting on Heat Transfer and Dynamics of Transient Cooling Processes with Liquid Film Flowing onto a Copper Plate. *J. Eng. Thermophys.* **2020**, *29*, 531–541. [CrossRef]
17. Orman, Ł.J.; Radek, N.; Pietraszek, J.; Szczepaniak, M. Analysis of Enhanced Pool Boiling Heat Transfer on Laser—Textured Surfaces. *Energies* **2020**, *13*, 2700. [CrossRef]
18. Voglar, J.; Gregorčič, P.; Zupančič, M.; Golobič, I. Boiling Performance on Surfaces with Capillary-Length-Spaced One- and Two-Dimensional Laser-Textured Patterns. *Int. J. Heat Mass Transf.* **2018**, *127*, 1188–1196. [CrossRef]
19. Zakšek, P.; Zupančič, M.; Gregorčič, P.; Golobič, I. Investigation of Nucleate Pool Boiling of Saturated Pure Liquids and Ethanol-Water Mixtures on Smooth and Laser-Textured Surfaces. *Nanosc. Microsc. Thermophys. Eng.* **2020**, *24*, 29–42. [CrossRef]
20. Serdyukov, V.; Starinskiy, S.; Malakhov, I.; Safonov, A.; Surtaev, A. Laser Texturing of Silicon Surface to Enhance Nucleate Pool Boiling Heat Transfer. *Appl. Therm. Eng.* **2021**, *194*, 117102. [CrossRef]
21. Kumar, G.U.; Suresh, S.; Kumar, C.S.; Back, S.; Kang, B.; Lee, H.J. A Review on The Role of Laser Textured Surfaces on Boiling Heat Transfer. *Appl. Therm. Eng.* **2020**, *174*, 115274. [CrossRef]
22. Kumar, A.; Hung, K.S.; Wang, C.C. Nucleate Pool Boiling Heat Transfer from High-Flux Tube with Dielectric Fluid HFE-7200. *Energies* **2020**, *13*, 2313. [CrossRef]
23. Liter, S.G.; Kaviany, M. Pool-Boiling CHF Enhancement by Modulated Porous-Layer Coating: Theory and Experiment. *Int. J. Heat Mass Transf.* **2001**, *44*, 4287–4311. [CrossRef]
24. Hwang, G.S.; Kaviany, M. Critical Heat Flux in Thin, Uniform Particle Coatings. *Int. J. Heat Mass Transf.* **2006**, *49*, 844–849. [CrossRef]
25. Min, D.H.; Hwang, G.S.; Usta, Y.; Cora, O.N.; Koc, M.; Kaviany, M. 2-D and 3-D Modulated Porous Coatings for Enhanced Pool Boiling. *Int. J. Heat Mass Transf.* **2009**, *52*, 2607–2613. [CrossRef]
26. Kalita, V.I.; Bocharova, M.A.; Trushnikova, A.S.; Shaternikov, B.N. Surface Structure of Titanium Materials Intended for Intraosseous Implants. *Russ. Metall. (Met.)* **2005**, *3*, 282–288.

27. Surtaev, A.S.; Pavlenko, A.N.; Kuznetsov, D.V.; Kalita, V.I.; Komlev, D.I.; Ivannikov, A.Y.; Radyuk, A.A. Heat Transfer and Crisis Phenomena at Pool Boiling of Liquid Nitrogen on the Surfaces with Capillary-Porous Coatings. *Int. J. Heat Mass Transf.* **2017**, *108*, 146–155. [CrossRef]
28. Surtaev, A.; Kuznetsov, D.; Serdyukov, V.; Pavlenko, A.; Kalita, V.; Komlev, D.; Radyuk, A.; Ivannikov, A. Structured Capillary-Porous Coatings for Enhancement of Heat Transfer at Pool Boiling. *Appl. Therm. Eng.* **2018**, *133*, 532–542. [CrossRef]
29. Pavlenko, A.N.; Kuznetsov, D.V.; Surtaev, A.S. Experimental Study of the Influence of Structured Capillary-Porous Coatings on the Dynamics of Development of Transient Processes and the Crisis Phenomena at Stepwise Heat Release. *J. Eng. Thermophys.* **2018**, *27*, 285–293. [CrossRef]
30. Cheng, H.C.; Jiang, Z.X.; Chang, T.L.; Chen, P.H. Effects of Difference in Wettability Level of Biphilic Patterns on Copper Tubes in Pool Boiling Heat Transfer. *Exp. Therm. Fluid Sci.* **2021**, *120*, 110241. [CrossRef]
31. Heidary, A.; Moghadasi, H.; Saffari, H. Impact of Dimensional Characteristics of Low-Conductive Channels on the Enhancement of Pool Boiling: An Experimental Analysis. *Int. J. Mech. Sci.* **2021**, *209*, 106710. [CrossRef]
32. Jaikumar, A.; Kandlikar, S.G. Enhanced Pool Boiling Heat Transfer Mechanisms for Selectively Sintered Open Microchannels. *Int. J. Heat Mass Transf.* **2015**, *88*, 652–661. [CrossRef]
33. Cho, H.R.; Park, S.C.; Kim, D.; Joo, H.M.; Yu, D.I. Experimental Study on Pool Boiling on Hydrophilic Micro/Nanotextured Surfaces with Hydrophobic Patterns. *Energies* **2021**, *14*, 7543. [CrossRef]
34. Zhukov, V.M.; Kuzma-Kichta, Y.A.; Lavrikov, A.V.; Belov, K.I.; Lenkov, V.A. Heat Transfer Investigation at Boiling of Nitrogen and Freon 113 on a Sphere with Coating Based on Al2O3 Obtained by Microarc Oxidation. *Therm. Process. Eng.* **2016**, *8*, 353–360.
35. Vasil'ev, N.V.; Varaksin, A.Y.; Zeigarnik, Y.A.; Khodakov, K.A. Characteristics of Subcooled Water Boiling on Structured Surfaces. *High Temp.* **2017**, *55*, 880–886. [CrossRef]
36. Pecherkin, N.; Pavlenko, A.; Volodin, O.; Kataev, A.; Mironova, I. Experimental Study of Heat Transfer Enhancement in a Falling Film of R21 on an Array of Horizontal Tubes with MAO Coating. *Int. Commun. Heat Mass Transf.* **2021**, *129*, 105743. [CrossRef]
37. Pavlenko, A.N.; Kuznetsov, D.V.; Bessmeltsev, V.P. Heat Transfer Enhancement during Pool Boiling of Nitrogen on Porous Coatings Produced by Selective Laser Melting/Sintering (SLM/SLS). *J. Eng. Thermophys.* **2022**, *31*, 1–10. [CrossRef]
38. Nikiforov, A.A.; Nikiforova, G.L.; Terleeva, O.P.; Slonova, A.I.; Eshchenko, V.N.; Li, D.K. Device for Micro-Electric Arc Oxidation. RU Patent C1 2248416, 20 March 2005.
39. Sheludyak, Y.E.; Kashporov, L.Y.; Malinin, L.A.; Calkov, V.N. *Thermophysical Properties of Combustible System Components*; NPO Inform TEI: Moscow, Russia, 1992; p. 36. (In Russian)
40. Kutateladze, S.S. On the Transition to Film Boiling under Natural Convection. *Kotloturbostroenie* **1948**, *3*, 10–12.
41. Zuber, N. Hydrodynamic Aspects of Boiling Heat Transfer. Ph.D. Thesis, University of California, Los Angeles, CA, USA, Ramo-Wooldridge Corporation, Los Angeles, CA, USA, 1959.
42. Verkin, B.I.; Kirichenko, Y.A.; Rusanov, K.V. *Heat Transfer during Boiling of Cryogenic Liquids*; Naukova Dumka: Kyiv, Ukrainian SSR, 1987; pp. 11–36. (In Russian)
43. Sychev, V.V.; Vasserman, A.A.; Kozlov, A.D.; Spiridonov, G.A.; Cymarkin, V.A. *Thermodynamic Properties of Nitrogen*; Izdatelstvo Standartov: Moscow, Ukrainian SSR, 1977; p. 145. (In Russian)
44. Cao, Z.; Wu, Z.; Sunden, B. Heat Transfer Prediction and Critical Heat Flux Mechanism for Pool Boiling of NOVEC-649 on Microporous Copper Surfaces. *Int. J. Heat Mass Transf.* **2019**, *141*, 818–834. [CrossRef]
45. Tang, K.; Bai, J.; Chen, S.; Zhang, S.; Li, J.; Sun, Y.; Chen, G. Pool Boiling Performance of Multilayer Micromeshes for Commercial High-Power Cooling. *Micromachines* **2021**, *12*, 980. [CrossRef]
46. Roizen, L.I.; Rachitskii, D.G.; Rubin, I.R.; Vertogradskaya, L.M.; Yudina, L.A.; Pypkina, M.B. Heat-Transfer with Boiling of Nitrogen and Freon-113 on Porous Metallic Coatings. *High Temp.* **1982**, *20*, 264–270.
47. Scurlock, R.G. Enhanced Boiling Heat Transfer Surfaces. *Cryogenics* **1995**, *35*, 233–237. [CrossRef]